© 2015. Published by The Company of Biologists Ltd | Development (2015) 142, 1978-1983 doi:10.1242/dev.122325

RESEARCH REPORT

DEFECTIVE KERNEL 1 promotes and maintains plant epidermal differentiation

Roberta Galletti[1,*], Kim L. Johnson[2], Simon Scofield[3], Rita San-Bento[1], Andrea M. Watt[2], James A. H. Murray[3] and Gwyneth C. Ingram[1,*]

ABSTRACT

During plant epidermal development, many cell types are generated from protodermal cells, a process requiring complex co-ordination of cell division, growth, endoreduplication and the acquisition of differentiated cellular morphologies. Here we show that the *Arabidopsis* phytocalpain DEFECTIVE KERNEL 1 (DEK1) promotes the differentiated epidermal state. Plants with reduced DEK1 activity produce cotyledon epidermis with protodermal characteristics, despite showing normal growth and endoreduplication. Furthermore, in non-embryonic tissues (true leaves, sepals), DEK1 is required for epidermis differentiation maintenance. We show that the HD-ZIP IV family of epidermis-specific differentiation-promoting transcription factors are key, albeit indirect, targets of DEK1 activity. We propose a model in which DEK1 influences HD-ZIP IV gene expression, and thus epidermis differentiation, by promoting cell adhesion and communication in the epidermis.

KEY WORDS: DEK1, Epidermis, Differentiation maintenance, *Arabidopsis thaliana*

INTRODUCTION

The production of specific function-adapted organ morphologies in plants is achieved by the exquisitely complex spatial and temporal control of cell proliferation, expansion and differentiation. The importance of this co-ordination is well illustrated in the cotyledon epidermis of *Arabidopsis thaliana*. To perform its basic functions this cell layer must produce both mature pavement cells (PCs), which can be very large and have a complex morphology, and appropriately spaced pairs of stomatal guard cells, which are tiny and adapted to their role in gas exchange (Glover, 2000). Producing this complex mosaic demands that neighbouring cells co-ordinate their growth.

Epidermal specification and differentiation are linked to the activity of subfamily IV of the plant-specific homeodomain-leucine zipper (HD-ZIP) transcription factors (TFs) (Abe et al., 2003; Depege-Fargeix et al., 2011; Di Cristina et al., 1996; Horstman et al., 2015; Javelle et al., 2011a, 2010; Nakamura et al., 2006; Peterson et al., 2013; Roeder et al., 2012; San-Bento et al., 2014; Takada et al., 2013; Vernoud et al., 2009; Wu et al., 2011; Yang et al., 2011). Cell-cell communication influences both epidermal cell fate decisions and subsequent differentiation (reviewed by Javelle et al., 2011b; Schiefelbein et al., 2014; Takada and Iida, 2014). For example, several receptor-like kinases (RLKs) and ligand-like peptides control patterning of the stomatal lineage (reviewed by Richardson and Torii, 2013) and the CRINKLY4 (CR4) RLK, and its *Arabidopsis* homologue ACR4, are required for the control of epidermal identity in maize (Becraft et al., 1996) and the expression of HD-ZIP IV genes in *Arabidopsis* (San-Bento et al., 2014).

DEFECTIVE KERNEL 1 (DEK1) regulates growth coordination and epidermal characters in plants (Becraft et al., 2002; Johnson et al., 2005, 2008; Lid et al., 2002). Loss of *DEK1* function causes early embryo lethality in both *Arabidopsis* and maize (Becraft et al., 2002; Johnson et al., 2005). In *Petunia* and *Arabidopsis*, strong downregulation of *DEK1* is accompanied by proliferation of disorganised callus-like cells (Ahn et al., 2004; Lid et al., 2005). *DEK1* is also required for multicellular development in the moss *Physcomitrella patens* (Demko et al., 2014; Liang et al., 2013; Perroud et al., 2014). DEK1 has a modular structure, with several predicted transmembrane domains, a linker domain and a cytoplasmically localised C-terminal domain comprising a sequence similar to animal calpains and a C2-like domain (Lid et al., 2002). The complete C-terminal domain (which we refer to as the CALPAIN domain) is sufficient to complement *dek1* loss-of-function alleles, suggesting that this is the active domain of the protein (Johnson et al., 2008; Liang et al., 2013). A weak *DEK1* allele, *dek1-4*, which causes a single amino acid substitution in the C2-like domain, and mutant alleles of *ACR4* and the HD-ZIP IV-encoding genes *HDG11* and *ATML1*, were recently reported to lack sepal giant cells (GCs) (Roeder et al., 2012).

Here we aim to understand the role of DEK1 in epidermis differentiation, and particularly to clarify its relationship with the HD-ZIP IV TFs.

RESULTS AND DISCUSSION

dek1-4 shows protodermal characteristics in cotyledon epidermis but no significant defects in cell expansion, ploidy or cell cycle-related gene expression

We found that the PCs in the adaxial epidermis of *dek1-4* were less complex and more homogeneous than in wild-type (WT; Col-0) controls (Fig. 1). Three-day-old Col-0 cotyledon PCs included small cells with almost no lobes, intermediate cells with few lobes and larger, fully interdigitated cells (Fig. 1A). At the same stage, *dek1-4* PCs ranged from showing no lobes (polygonal shape) to showing some interdigitation, although less than in Col-0 (Fig. 1B,C). We noted an abnormally high frequency of four-way, or near four-way, junctions (usually found in meristematic cells) in *dek1-4* (Fig. 1B,C).

In the *dek1-4* mutant, intermediate size and large cells were rounder than WT cells of similar size (Fig. 1D). Despite their shape differences, the average final cell size of PCs in *dek1-4* and WT was similar (Fig. 1E). Thus, PCs in *dek1-4* have, on average, less complex shapes. This cellular phenotype persisted in fully expanded cotyledons (Fig. 1H,I). Neighbouring PCs in *dek1-4* frequently had shared

[1]Laboratoire de Reproduction et Développement des Plantes, Ecole Normale Supérieure de Lyon, 46 allée d'Italie, Lyon 69364, Cedex 07, France. [2]ARC Centre of Excellence in Plant Cell Walls, School of Botany, University of Melbourne, Royal Parade, Parkville, Victoria 3010, Australia. [3]Cardiff School of Biosciences, Cardiff University, Museum Avenue, Cardiff CF10 3AX, UK.

*Authors for correspondence (roberta.galletti@ens-lyon.fr; gwyneth.ingram@ens-lyon.fr)

Received 19 January 2015; Accepted 7 April 2015

Development (2015) 142, 1978-1983 doi:10.1242/dev.122325

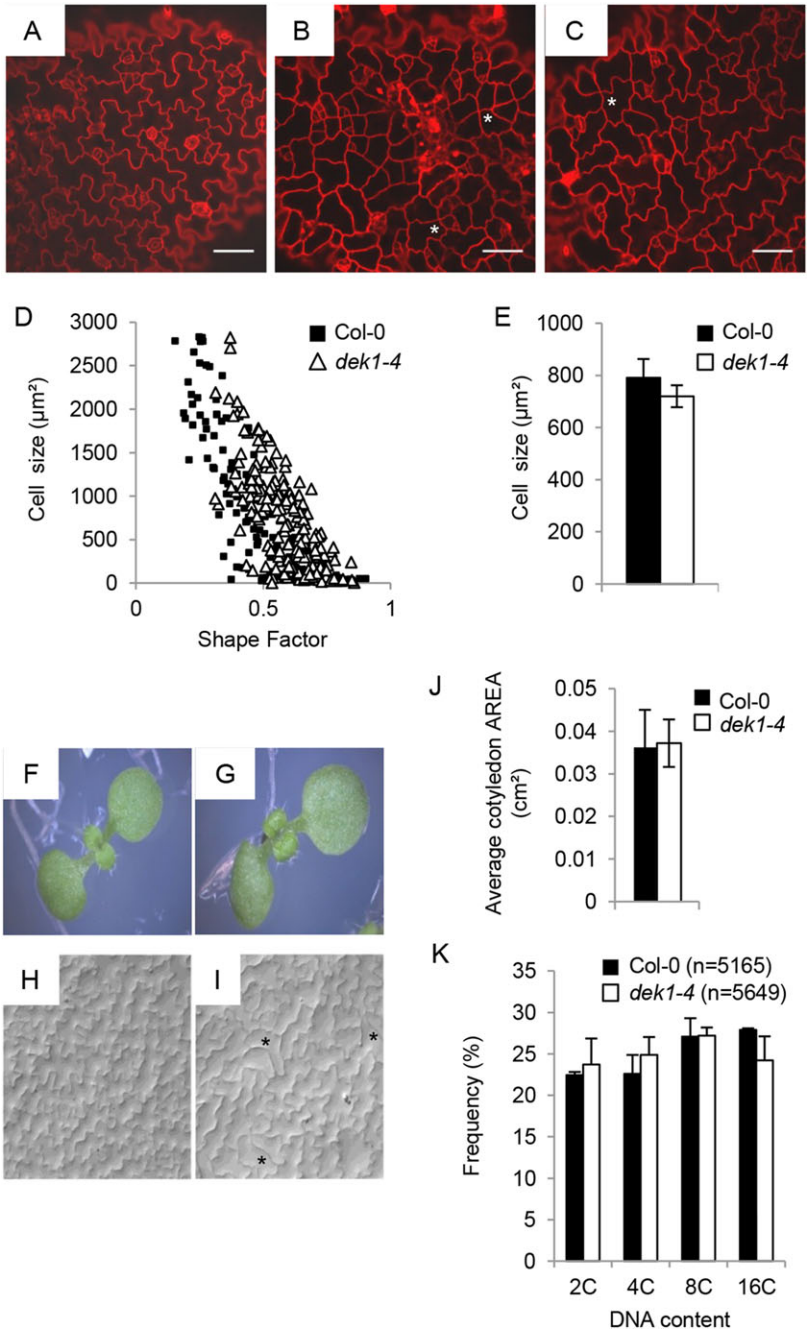

Fig. 1. DEK1 promotes cell differentiation. (A-C) Confocal images of the adaxial side of 3-day-old Col-0 (A) and *dek1-4* (B,C) *Arabidopsis* cotyledons stained with PI. Scale bars: 50 µm. (D) Epidermal cell area plotted against shape factor (combined data from cells measured in four independent seedlings). Guard cells were eliminated from the analysis. n=135 for Col-0 and n=189 for *dek1-4*. (E) Average area±s.e. of epidermal pavement cells (PCs). (F-I) Images and agarose imprints of the adaxial side of 8-day-old Col-0 (F,H) and *dek1-4* (G,I) seedlings. Asterisks indicate four-way junctions (B,C) or neighbouring PCs with shared straight cell walls (I) in the mutant. (J) Average area±s.e. of 8-day-old cotyledons. n=19 for Col-0 and n=16 for *dek1-4*. (K) Nuclear DNA content/ploidy distribution profile of 10-day-old Col-0 and *dek1-4* cotyledons. n=nuclei counted per sample.

straight walls (Fig. 1I) suggesting that they had undergone late divisions (observed in 100% of mutant seedlings, but only twice in 40 WT seedlings analysed). No defect in blade expansion was observed (Fig. 1J), but cotyledons were frequently epinastically curled (Fig. 1G).

Leaf blade curling was described in *CYCLIN D3;1* (*CYCD3;1*)-overexpressing plants, where it was associated with dramatic changes in ploidy distribution (Scofield et al., 2013). However, no significant differences in ploidy distribution were detected between WT and *dek1-4* cotyledons (Fig. 1K). Consistent with this, no differences in the expression of *CYCD3;1*, or other cell cycle-related genes such as *LOSS OF GIANT CELLS FROM ORGANS* (*LGO*), *SIAMESE* (*SIM*), *KIP-RELATED PROTEIN 6* (*KRP6*), *HOBBIT* (*HBT*) or *DEL1*, which encodes an endocycle inhibiting E2F-like protein, were observed between Col-0 and *dek1-4* seedlings (supplementary material Fig. S1). Therefore, the phenotypes observed are not associated with ploidy defects.

DEK1 controls epidermal differentiation via a pathway involving multiple HD-ZIP IV-encoding genes

dek1-4 leaves showed a significantly higher proportion of trichomes with more than three branches than WT controls (Wilcoxon rank sum test, P=1.7^{-20}) (Fig. 2A-C). A similar phenotype was described for *hdg11* and *hdg12 hdg11* mutants (Nakamura et al., 2006). We analysed the expression of *HDG11*, *HDG12* and of additional HD-ZIP IV genes (*ATML1*, *PDF2*, *HDG2*) in the *dek1-4* mutant and found that all genes tested were reproducibly downregulated (Fig. 2D). We then assessed the genetic relationship between *DEK1*, *HDG11* and *HDG12*. *hdg12-2 dek1-4* double mutants showed highly branched trichomes, as seen in the *dek1-4* parental

Development (2015) 142, 1978-1983 doi:10.1242/dev.122325

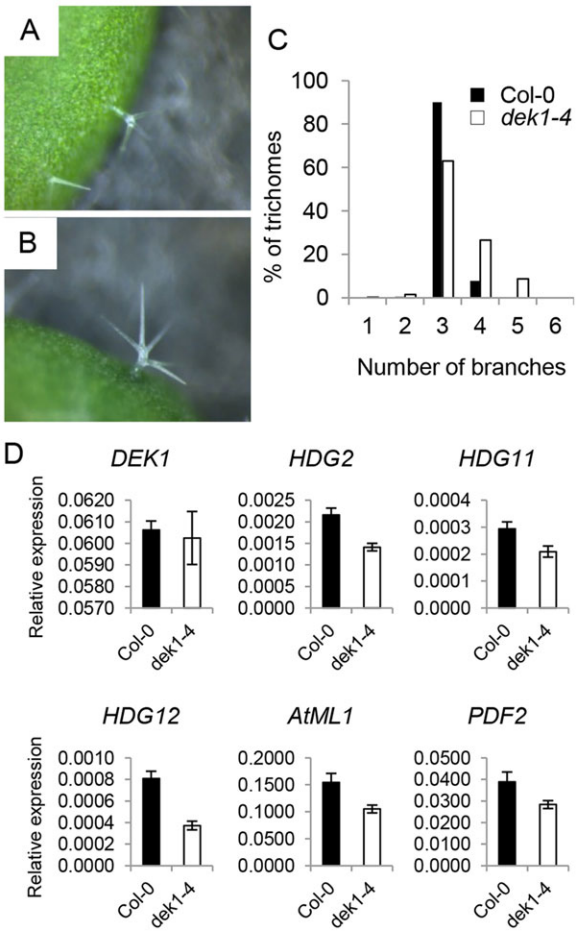

Fig. 2. *dek1-4* mutants show reduced expression of differentiation-promoting HD-ZIP IV TF-encoding genes. (A,B) Ten-day-old Col-0 (A) and *dek1-4* (B) seedlings. (C) Distribution of branch point numbers in the first and second true leaves of 15-day-old plants. Number of trichomes: n=500 for Col-0 and n=400 for *dek1-4*. (D) Gene expression levels in 6-day-old Col-0 and *dek1-4* seedlings were quantified by qRT-PCR and normalised using the expression of *EIF4A*. Shown is the average of three independent biological replicates±s.d.

line, but did not exhibit additional defects. In *dek1-4 hdg11-2* plants we observed no significant additivity of the trichome phenotypes of the two mutants (supplementary material Fig. S2). The sepals of *hdg12-2 dek1-4* and of *dek1-4 hdg11-2* mutants resembled those of *dek1-4* mutants (supplementary material Fig. S3). Together, our results are consistent with multiple HD-ZIP IV proteins acting downstream of DEK1 to regulate epidermal differentiation.

To confirm whether the phenotype of the *dek1-4* allele is caused by reduced DEK1 activity, we expressed an artificial microRNA (Ossowski et al., 2008) targeted to the *DEK1* coding sequence (*amiRDEK1*) under the CaMV 35S promoter and under a dexamethasone (DEX)-inducible promoter (Craft et al., 2005; Samalova et al., 2005). T1 *35S:amiRDEK1* plants showed similar phenotypes to those reported for *AtDEK1RNAi* lines (Johnson et al., 2005) and the *dek1-4* mutant (Roeder et al., 2012). Some seedlings had fused cotyledons, discontinuous epidermis and died. Surviving seedlings had PCs with shallow lobes, true leaves with multi-branched trichomes, twisted rosette leaves with elongated petioles and sepals devoid of GCs (supplementary material Fig. S4). Three independent homozygous lines showing reduced expression levels of *DEK1* (Fig. 3A) were analysed. The expression levels of all HD-ZIP IV genes previously analysed were not only reduced, but also correlated tightly with the levels of *DEK1* transcript (Fig. 3A) and with the severity of PC phenotypes (Fig. 3B) and trichome branching defects (Wilcoxon rank sum test: P=4.24^{-23} for line C, P=3.03^{-23} for line L) (Fig. 3C). Aborted trichomes were observed (Fig. 3D) but not included in the statistical analysis.

To study the effects of overexpressing the active form of DEK1 (the CALPAIN domain) on the expression of HD-ZIP IV genes, we used transgenic seedlings harbouring a *pRPS5A:CALPAIN-6XHIS* construct (*OEX [WT]*). Endogenous levels of *DEK1* were similar to that of WT plants, but *CALPAIN* transcript levels (transgene+ endogenous) were several times higher than in Col-0 seedlings (supplementary material Fig. S5). No consistent changes in the expression of HD-ZIP IV genes were observed in these lines compared with WT seedlings (supplementary material Fig. S5), suggesting that HD-ZIP IV gene regulation by DEK1 is either indirect or requires additional factors.

Fine-tuned silencing of *DEK1* expression leads to the appearance of dividing GC-like structures in sepals

Two independent homozygous lines in which *amiRDEK1* expression was triggered only upon DEX application were selected. Induction of *amiRDEK1* expression lowered *DEK1* mRNA levels to about half those detected in control plants (supplementary material Fig. S4J). Upon flowering, control sepals showed a classic epidermal structure with GCs surrounded by smaller cells (Fig. 4A). In DEX-grown plants, we observed sepals with few or no GCs, as well as GC-like structures that had undergone late divisions after the onset of differentiation (Fig. 4B-D). Thus, reduced levels of DEK1 affect the maintenance of GC differentiation.

Cell shape defects in *dek1-4* are not caused by changes in microtubule behaviour

PC shape is affected in mutants with altered cortical microtubule (CMT) dynamics (Ivakov and Persson, 2013). The *dek1-4* allele was introgressed into a line harbouring a GFP-TUA6 expression construct (Ueda et al., 1999) and the resulting plants analysed. In WT seedlings, small polygonal PCs have highly oriented CMTs arranged transversely with respect to their long axis, while in more lobed PCs CMTs usually orient more randomly and bundle densely in neck regions. In *dek1-4*, CMTs are mainly oriented perpendicularly to the long axis of the cell (supplementary material Fig. S6B,C). Quantification confirmed that CMTs in mutant PCs are more highly oriented than in WT PCs (supplementary material Fig. S6D).

To test whether their abnormal arrangement in the mutant was due to an inability of CMTs to rearrange their distribution, or was a consequence of cell shape defects, we studied CMT reorganisation upon ablation in cotyledons (Sampathkumar et al., 2014). CMTs in both mutant and WT cotyledons reoriented in cell files surrounding the ablation site (supplementary material Fig. S6E-H), suggesting that CMT dynamics are not disrupted in *dek1-4*. This observation supports the hypothesis that the CMT arrangement in the mutant is a consequence of altered cell shape.

DEK1 activity may define epidermal cell-cell contact zones

A recent study has provided strong evidence that the expression of HD-ZIP IV-encoding genes is maintained by intercellular signalling mediated by ACR4 (San-Bento et al., 2014). We measured the height of epidermal cell contact zones and found that they are less uniform in height in *dek1-4* than in WT seedlings (supplementary material Fig. S7). Consistent with a defect in epidermal cell adhesion (Singh et al., 2005), we also observed examples of cell separation in the cotyledons of *35S:amiRDEK1* lines and the abnormal accumulation of callose at epidermal cell boundaries in

Development (2015) 142, 1978-1983 doi:10.1242/dev.122325

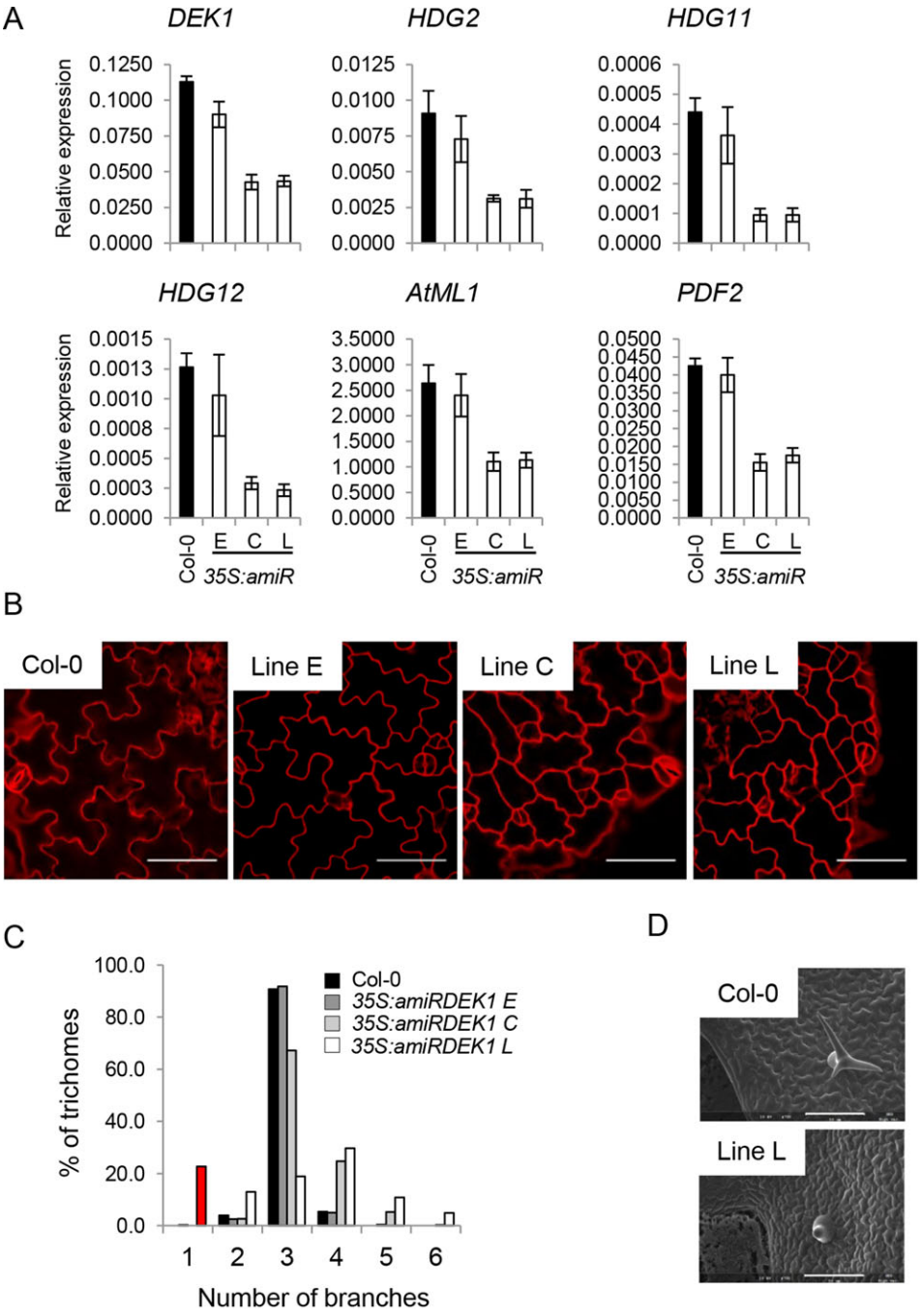

Fig. 3. *DEK1* transcript levels correlate with HD-ZIP IV gene expression and with epidermal phenotypes. (A) Gene expression levels in the aerial parts of 6-day-old Col-0 and *35S:amiRDEK1* seedlings were quantified by qRT-PCR and normalised using the expression of *EIF4A*. Shown is the average of three independent biological replicates±s.d. (B) Confocal images of the adaxial side of 4-day-old cotyledons stained with PI. Scale bars: 50 µm. (C) Distribution of branch point numbers in the first and second true leaves of 15-day-old plants. Number of trichomes: *n*=507 for Col-0, *n*=515 for line E, *n*=498 for line C and *n*=143 for line L. Red bar, aborted trichomes. (D) Scanning electron micrographs of true leaves from 15-day-old plants. Scale bars: 50 µm.

the expanding cotyledons of *dek1-4* seedlings (supplementary material Fig. S7).

Unlike animal calpains, which exist in many isoforms, *DEK1* is a single-copy gene unique to land plants (Liang et al., 2013; Lid et al., 2002). Here we show that defects in DEK1 perturb epidermal cell differentiation via a mechanism affecting the transcription of genes encoding HD-ZIP IV family TFs. The ancestral HD-ZIP IV protein, like DEK1, is thought to have arisen in the common algal ancestor of land plants, where it might have been crucial in the evolution of a specialised outer cell layer with the characteristics necessary for life on land, such as cuticle formation and stomatal development (Zalewski et al., 2013). Apoplastic signalling mediated by ACR4, like DEK1 function, is necessary for the maintenance of HD-ZIP IV gene expression (San-Bento et al., 2014). However, genetic analysis carried out in *Arabidopsis* and maize (Becraft et al., 2002; Roeder et al., 2012) suggests that DEK1 and ACR4 act in parallel.

A key requirement of the epidermis is that it should be continuous, implying the maintenance of a highly regulated zone of circumferential contact between neighbouring cells. A common feature of phenotypes associated with loss of DEK1 activity is epidermal cell separation, suggesting that DEK1 might regulate this zone of cell-cell contact (Ahn et al., 2004; Johnson et al., 2005; Lid et al., 2005). Here we show that although *dek1-4* mutants produce a continuous epidermis, the zone of cell-cell contact between epidermal cells is perturbed, further supporting this hypothesis. We propose that DEK1 influences HD-ZIP IV gene expression, and thus epidermal differentiation, by regulating epidermal cell adhesion, a function that might have been crucial in the successful move of plants onto dry land.

Development (2015) 142, 1978-1983 doi:10.1242/dev.122325

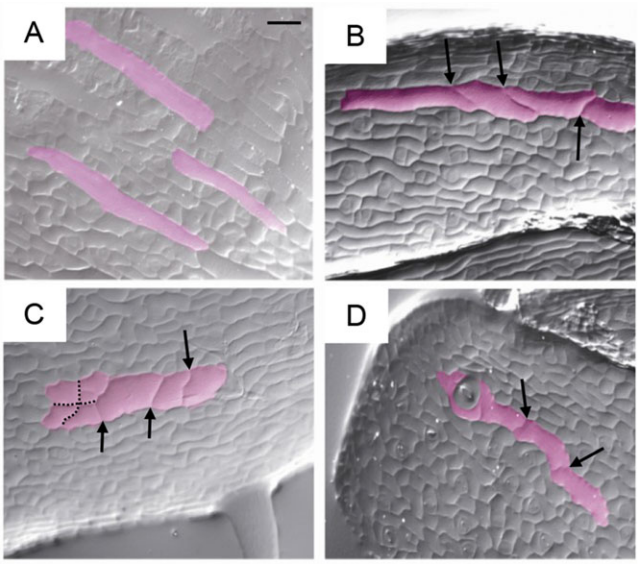

Fig. 4. Silencing of the *DEK1* gene leads to the appearance of dividing GCs in sepals. Agarose imprints of sepal epidermis from DEX-grown Col-0 (A) and *amiRDEK1* line 2 (B,C) and 3 (D) plants. GCs are false coloured in pink. Arrows indicate divisions that have occurred in GCs; dotted lines indicate common division planes in a group of cells. Scale bar: 50 µm.

MATERIALS AND METHODS

Plant material and growth conditions

Seeds were obtained from the Nottingham Arabidopsis Stock Centre unless otherwise stated. The *dek1-4* allele was donated by Adrienne Roeder (Cornell University, USA) and introgressed into the Col-0 background. *dek1-4* genotyping involved amplifying genomic DNA using the primers shown in supplementary material Table S1 and sequencing the resulting product with primer RG15 (supplementary material Table S1, Fig. S2). T-DNA insertion lines were genotyped using the primers described in supplementary material Table S1. A *DEK1*-specific artificial microRNA was designed using MicroRNA Designer (WMD, http://wmd3.weigelworld.org) and generated using the PCR primers in supplementary material Table S1 according to the protocol from WMD. The *pre-amiRNA* was recombined into pDONR221 (Invitrogen) and then into the Gateway-compatible binary vector pART27 (Lee and Gelvin, 2008) under control of a CaMV 35S promoter, or into the pOPON2.1 vector (a gift from Ian Moore, University of Oxford, UK). Plants expressing *pRPS5A:CALPAIN-6XHIS* were generated as described for *pRPS5A:CALPAIN-GFP* (Johnson et al., 2008), but with the insertion of an in-frame two times 6×His tag with a STOP codon in place of the *GFP* sequence.

Soil-grown plants were placed at 20°C and 55% relative humidity under a 16-h light/8-h dark cycle. For *in vitro* cultures, seeds were surface sterilised with chlorine gas, stratified on media for 2-3 days in the dark and germinated under a 16-h light/8-h dark cycle at 21°C. To induce *DEK1* silencing, germinated seedlings were transferred after 5 days onto medium supplemented with 0.4% DMSO (as control) or 25 µm dexamethasone (DEX).

Imaging and image analysis

Scanning electron microscopy samples were mounted on graphite paste (Electron Microscopy Sciences) and visualised using an SH-3000 table-top scanning electron microscope (HIROX) at −30°C or −50°C with an accelerating voltage of 5 kV.

Cotyledon PC cell walls were stained with 1 mg/ml propidium iodide (PI) for 5 min, briefly rinsed, and imaged at a point midway between the midrib and margin and halfway along the blade. Cell areas and perimeters were measured using ImageJ (NIH). A 'shape factor' ($SF=4\pi$ area/perimeter^2) was calculated for each cell (Dewitte et al., 2007). CMT alignments were quantified using the ImageJ plug-in FibrilTool (Boudaoud et al., 2014). All confocal images were acquired using an LSM700 confocal microscope (Carl Zeiss).

For tissue imprints, we used an agarose-based method (Mathur and Koncz, 1997). Light micrographs were taken with an Axio Imager.M2 microscope (Carl Zeiss) using DIC optics.

RNA extraction and quantitative gene expression analysis

Seedlings were grown vertically for 6 days on square plates and aerial parts harvested. Three independent biological replicates of 15-20 seedlings were used. RNA extraction, DNase treatment and qPCR analysis were carried out as described previously (Xing et al., 2013). Expression levels of each gene, relative to *EIF4A*, were determined as previously described (Ferrari et al., 2006). Primers used for qRT-PCR analysis are shown in supplementary material Table S1.

Ploidy analysis

Cotyledons were harvested with forceps, chopped with a razor blade in nuclear lysis buffer (Dewitte et al., 2007), filtered and stained with DAPI. The nuclei-containing solution was analysed with a Partec ploidy analyser. Three biological replicates (20 cotyledons from ten independent plants for each replicate) were performed.

Acknowledgements

We thank Adrienne Roeder (Cornell University, USA) for providing the original *dek1-4* mutant line and for helpful discussions; Ian Moore (University of Oxford, UK) for providing the binary vector pOPON2.1; and Jeremy Just (RDP, ENS de Lyon, France) for helping with statistical analysis.

Competing interests

The authors declare no competing or financial interests.

Author contributions

R.G. and G.C.I. designed the experiments and wrote the paper; R.G., G.C.I., S.S. and A.M.W. performed the experiments; K.L.J. and R.S.-B. generated materials; J.A.H.M. contributed analytic tools.

Funding

R.G. was supported by an Agence Nationale de la Recherche (France) Chaire D' Excellence [ANR-10-CHEX-0011 - 01 to G.C.I.], R.S.-B. by the Marie Curie ITN SIREN, and A.M.W. by a Victorian Government postdoctoral training fellowship.

Supplementary material

Supplementary material available online at
http://dev.biologists.org/lookup/suppl/doi:10.1242/dev.122325/-/DC1

References

Abe, M., Katsumata, H., Komeda, Y. and Takahashi, T. (2003). Regulation of shoot epidermal cell differentiation by a pair of homeodomain proteins in Arabidopsis. *Development* **130**, 635-643.

Ahn, J.-W., Kim, M., Lim, J. H., Kim, G.-T. and Pai, H.-S. (2004). Phytocalpain controls the proliferation and differentiation fates of cells in plant organ development. *Plant J.* **38**, 969-981.

Becraft, P. W., Stinard, P. S. and McCarty, D. R. (1996). CRINKLY4: a TNFR-like receptor kinase involved in maize epidermal differentiation. *Science* **273**, 1406-1409.

Becraft, P. W., Li, K., Dey, N. and Asuncion-Crabb, Y. (2002). The maize dek1 gene functions in embryonic pattern formation and cell fate specification. *Development* **129**, 5217-5225.

Boudaoud, A., Burian, A., Borowska-Wykręt, D., Uyttewaal, M., Wrzalik, R., Kwiatkowska, D. and Hamant, O. (2014). FibrilTool, an ImageJ plug-in to quantify fibrillar structures in raw microscopy images. *Nat. Protoc.* **9**, 457-463.

Craft, J., Samalova, M., Baroux, C., Townley, H., Martinez, A., Jepson, I., Tsiantis, M. and Moore, I. (2005). New pOp/LhG4 vectors for stringent glucocorticoid-dependent transgene expression in Arabidopsis. *Plant J.* **41**, 899-918.

Demko, V., Perroud, P.-F., Johansen, W., Delwiche, C. F., Cooper, E. D., Remme, P., Ako, A. E., Kugler, K. G., Mayer, K. F. X., Quatrano, R. et al. (2014). Genetic analysis of DEFECTIVE KERNEL1 loop function in three-dimensional body patterning in Physcomitrella patens. *Plant Physiol.* **166**, 903-919.

Depege-Fargeix, N., Javelle, M., Chambrier, P., Frangne, N., Gerentes, D., Perez, P., Rogowsky, P. M. and Vernoud, V. (2011). Functional characterization of the HD-ZIP IV transcription factor OCL1 from maize. *J. Exp. Bot.* **62**, 293-305.

Dewitte, W., Scofield, S., Alcasabas, A. A., Maughan, S. C., Menges, M., Braun, N., Collins, C., Nieuwland, J., Prinsen, E., Sundaresan, V. et al. (2007). Arabidopsis CYCD3 D-type cyclins link cell proliferation and endocycles and

are rate-limiting for cytokinin responses. *Proc. Natl. Acad. Sci. USA* **104**, 14537-14542.
Di Cristina, M., Sessa, G., Dolan, L., Linstead, P., Baima, S., Ruberti, I. and Morelli, G. (1996). The Arabidopsis Athb-10 (GLABRA2) is an HD-Zip protein required for regulation of root hair development. *Plant J.* **10**, 393-402.
Ferrari, S., Galletti, R., Vairo, D., Cervone, F. and De Lorenzo, G. (2006). Antisense expression of the Arabidopsis thaliana AtPGIP1 gene reduces polygalacturonase-inhibiting protein accumulation and enhances susceptibility to Botrytis cinerea. *Mol. Plant Microbe Interact.* **19**, 931-936.
Galletti, R., Denoux, C., Gambetta, S., Dewdney, J., Ausubel, F. M., De Lorenzo, G. and Ferrari, S. (2008). The AtrbohD-mediated oxidative burst elicited by oligogalacturonides in Arabidopsis is dispensable for the activation of defense responses effective against Botrytis cinerea. *Plant Physiol.* **148**, 1695-1706.
Glover, B. J. (2000). Differentiation in plant epidermal cells. *J. Exp. Bot.* **51**, 497-505.
Horstman, A., Fukuoka, H., Muino, J. M., Nitsch, L., Guo, C., Passarinho, P., Sanchez-Perez, G., Immink, R., Angenent, G. and Boutilier, K. (2015). AIL and HDG proteins act antagonistically to control cell proliferation. *Development* **142**, 454-464.
Ivakov, A. and Persson, S. (2013). Plant cell shape: modulators and measurements. *Front. Plant Sci.* **4**, 439.
Javelle, M., Vernoud, V., Depege-Fargeix, N., Arnould, C., Oursel, D., Domergue, F., Sarda, X. and Rogowsky, P. M. (2010). Overexpression of the epidermis-specific homeodomain-leucine zipper IV transcription factor Outer Cell Layer1 in maize identifies target genes involved in lipid metabolism and cuticle biosynthesis. *Plant Physiol.* **154**, 273-286.
Javelle, M., Klein-Cosson, C., Vernoud, V., Boltz, V., Maher, C., Timmermans, M., Depege-Fargeix, N. and Rogowsky, P. M. (2011a). Genome-wide characterization of the HD-ZIP IV transcription factor family in maize: preferential expression in the epidermis. *Plant Physiol.* **157**, 790-803.
Javelle, M., Vernoud, V., Rogowsky, P. M. and Ingram, G. C. (2011b). Epidermis: the formation and functions of a fundamental plant tissue. *New Phytol.* **189**, 17-39.
Johnson, K. L., Degnan, K. A., Ross Walker, J. and Ingram, G. C. (2005). AtDEK1 is essential for specification of embryonic epidermal cell fate. *Plant J.* **44**, 114-127.
Johnson, K. L., Faulkner, C., Jeffree, C. E. and Ingram, G. C. (2008). The phytocalpain defective kernel 1 is a novel Arabidopsis growth regulator whose activity is regulated by proteolytic processing. *Plant Cell* **20**, 2619-2630.
Lee, L.-Y. and Gelvin, S. B. (2008). T-DNA binary vectors and systems. *Plant Physiol.* **146**, 325-332.
Liang, Z., Demko, V., Wilson, R. C., Johnson, K. A., Ahmad, R., Perroud, P.-F., Quatrano, R., Zhao, S., Shalchian-Tabrizi, K., Otegui, M. S. et al. (2013). The catalytic domain CysPc of the DEK1 calpain is functionally conserved in land plants. *Plant J.* **75**, 742-754.
Lid, S. E., Gruis, D., Jung, R., Lorentzen, J. A., Ananiev, E., Chamberlin, M., Niu, X., Meeley, R., Nichols, S. and Olsen, O.-A. (2002). The *defective kernel 1* (*dek1*) gene required for aleurone cell development in the endosperm of maize grains encodes a membrane protein of the calpain gene superfamily. *Proc. Natl. Acad. Sci. USA* **99**, 5460-5465.
Lid, S. E., Olsen, L., Nestestog, R., Aukerman, M., Brown, R. C., Lemmon, B., Mucha, M., Opsahl-Sorteberg, H.-G. and Olsen, O.-A. (2005). Mutation in the Arabidopsis thaliana DEK1 calpain gene perturbs endosperm and embryo development while over-expression affects organ development globally. *Planta* **221**, 339-351.
Mathur, J. and Koncz, C. (1997). Method for preparation of epidermal imprints using agarose. *Biotechniques* **22**, 280-282.
Nakamura, M., Katsumata, H., Abe, M., Yabe, N., Komeda, Y., Yamamoto, K. T. and Takahashi, T. (2006). Characterization of the class IV homeodomain-leucine zipper gene family in Arabidopsis. *Plant Physiol.* **141**, 1363-1375.
Ossowski, S., Schwab, R. and Weigel, D. (2008). Gene silencing in plants using artificial microRNAs and other small RNAs. *Plant J.* **53**, 674-690.
Perroud, P.-F., Demko, V., Johansen, W., Wilson, R. C., Olsen, O.-A. and Quatrano, R. S. (2014). Defective Kernel 1 (DEK1) is required for three-dimensional growth in Physcomitrella patens. *New Phytol.* **203**, 794-804.
Peterson, K. M., Shyu, C., Burr, C. A., Horst, R. J., Kanaoka, M. M., Omae, M., Sato, Y. and Torii, K. U. (2013). Arabidopsis homeodomain-leucine zipper IV proteins promote stomatal development and ectopically induce stomata beyond the epidermis. *Development* **140**, 1924-1935.
Richardson, L. G. L. and Torii, K. U. (2013). Take a deep breath: peptide signalling in stomatal patterning and differentiation. *J. Exp. Bot.* **64**, 5243-5251.
Roeder, A. H. K., Cunha, A., Ohno, C. K. and Meyerowitz, E. M. (2012). Cell cycle regulates cell type in the Arabidopsis sepal. *Development* **139**, 4416-4427.
Samalova, M., Brzobohaty, B. and Moore, I. (2005). pOp6/LhGR: a stringently regulated and highly responsive dexamethasone-inducible gene expression system for tobacco. *Plant J.* **41**, 919-935.
Sampathkumar, A., Krupinski, P., Wightman, R., Milani, P., Berquand, A., Boudaoud, A., Hamant, O., Jönsson, H. and Meyerowitz, E. M. (2014). Subcellular and supracellular mechanical stress prescribes cytoskeleton behavior in Arabidopsis cotyledon pavement cells. *Elife* **3**, e01967.
San-Bento, R., Farcot, E., Galletti, R., Creff, A. and Ingram, G. (2014). Epidermal identity is maintained by cell-cell communication via a universally active feedback loop in Arabidopsis thaliana. *Plant J.* **77**, 46-58.
Schiefelbein, J., Huang, L. and Zheng, X. (2014). Regulation of epidermal cell fate in Arabidopsis roots: the importance of multiple feedback loops. *Front. Plant Sci.* **5**, 47.
Scofield, S., Dewitte, W., Nieuwland, J. and Murray, J. A. H. (2013). The Arabidopsis homeobox gene SHOOT MERISTEMLESS has cellular and meristem-organisational roles with differential requirements for cytokinin and CYCD3 activity. *Plant J.* **75**, 53-66.
Singh, S. K., Eland, C., Harholt, J., Scheller, H. V. and Marchant, A. (2005). Cell adhesion in Arabidopsis thaliana is mediated by ECTOPICALLY PARTING CELLS 1–a glycosyltransferase (GT64) related to the animal exostosins. *Plant J.* **43**, 384-397.
Takada, S. and Iida, H. (2014). Specification of epidermal cell fate in plant shoots. *Front. Plant Sci.* **5**, 49.
Takada, S., Takada, N. and Yoshida, A. (2013). ATML1 promotes epidermal cell differentiation in Arabidopsis shoots. *Development* **140**, 1919-1923.
Ueda, K., Matsuyama, T. and Hashimoto, T. (1999). Visualization of microtubules in living cells of transgenic Arabidopsis thaliana. *Protoplasma* **206**, 201-206.
Vernoud, V., Laigle, G., Rozier, F., Meeley, R. B., Perez, P. and Rogowsky, P. M. (2009). The HD-ZIP IV transcription factor OCL4 is necessary for trichome patterning and anther development in maize. *Plant J.* **59**, 883-894.
Wu, R., Li, S., He, S., Wassmann, F., Yu, C., Qin, G., Schreiber, L., Qu, L.-J. and Gu, H. (2011). CFL1, a WW domain protein, regulates cuticle development by modulating the function of HDG1, a class IV homeodomain transcription factor, in rice and Arabidopsis. *Plant Cell* **23**, 3392-3411.
Xing, Q., Creff, A., Waters, A., Tanaka, H., Goodrich, J. and Ingram, G. C. (2013). ZHOUPI controls embryonic cuticle formation via a signalling pathway involving the subtilisin protease ABNORMAL LEAF-SHAPE1 and the receptor kinases GASSHO1 and GASSHO2. *Development* **140**, 770-779.
Yang, C., Li, H., Zhang, J., Luo, Z., Gong, P., Zhang, C., Li, J., Wang, T., Zhang, Y., Lu, Y. et al. (2011). A regulatory gene induces trichome formation and embryo lethality in tomato. *Proc. Natl. Acad. Sci. USA* **108**, 11836-11841.
Zalewski, C. S., Floyd, S. K., Furumizu, C., Sakakibara, K., Stevenson, D. W. and Bowman, J. L. (2013). Evolution of the class IV HD-zip gene family in streptophytes. *Mol. Biol. Evol.* **30**, 2347-2365.

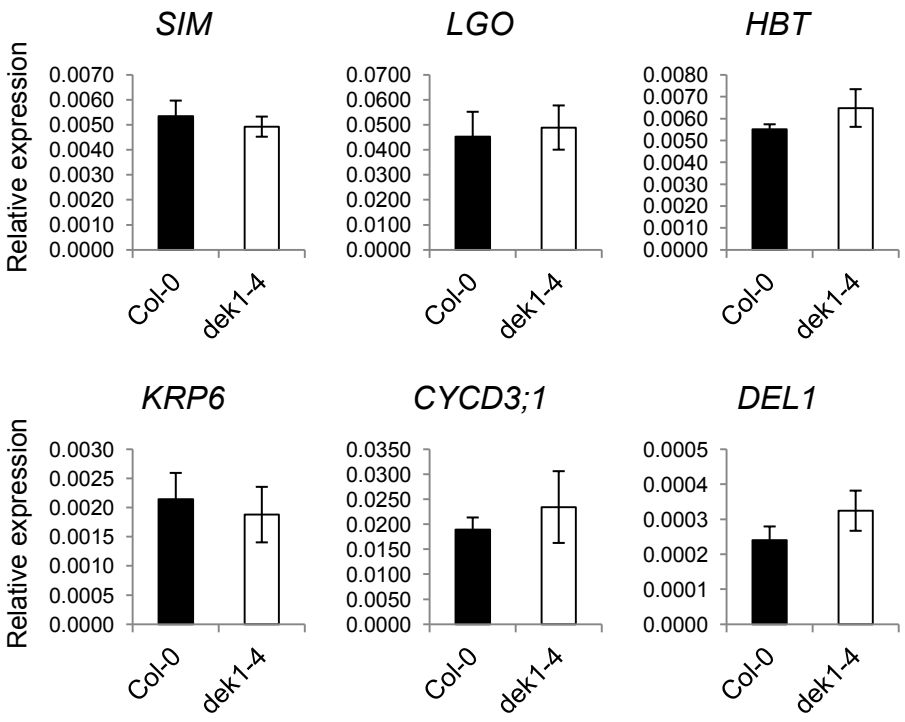

Figure S1 - *DEK1* activity does not directly affect the expression of cell cycle-related genes.

Gene expression levels in the aerial parts of 6-day-old Col-0 and *dek1-4* seedlings were quantified by qRT-PCR and normalized using the expression of the *EIF4A* gene. Graph represents the average of three independent biological replicates ± SD.

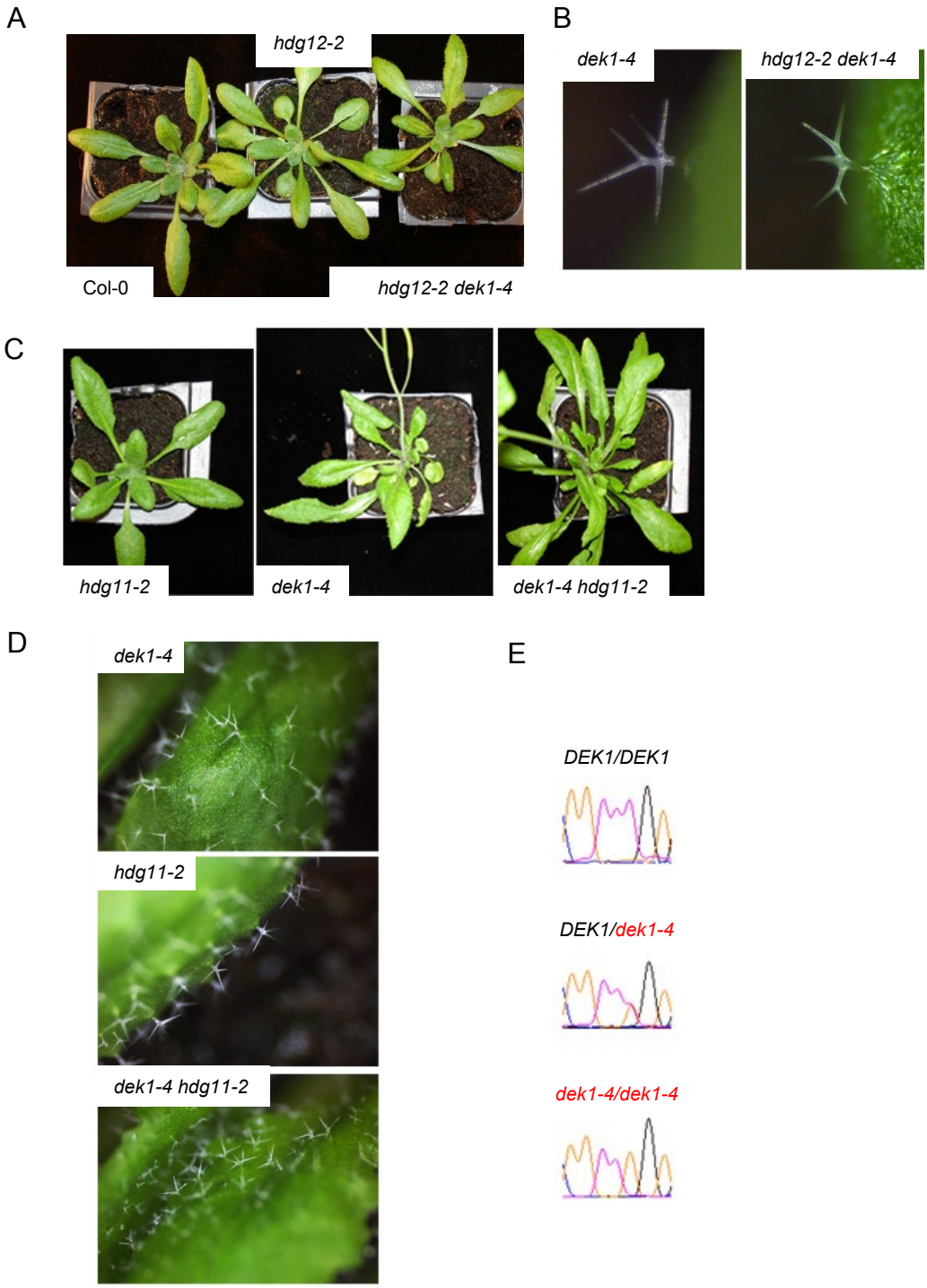

Figure S2- Phenotypic characterization of *hdg11-2, hdg12-2* and double mutants with *dek1-4*.

Phenotypes of double *hdg12-2 dek1-4* mutant plants (**A**) and trichomes (**B**). Phenotypes of double *dek1-4 hdg11-2* mutant plants (**C**) and trichomes (**D**). (**E**) Typical chromotograms produced during genotyping for the *dek1-4* allele.

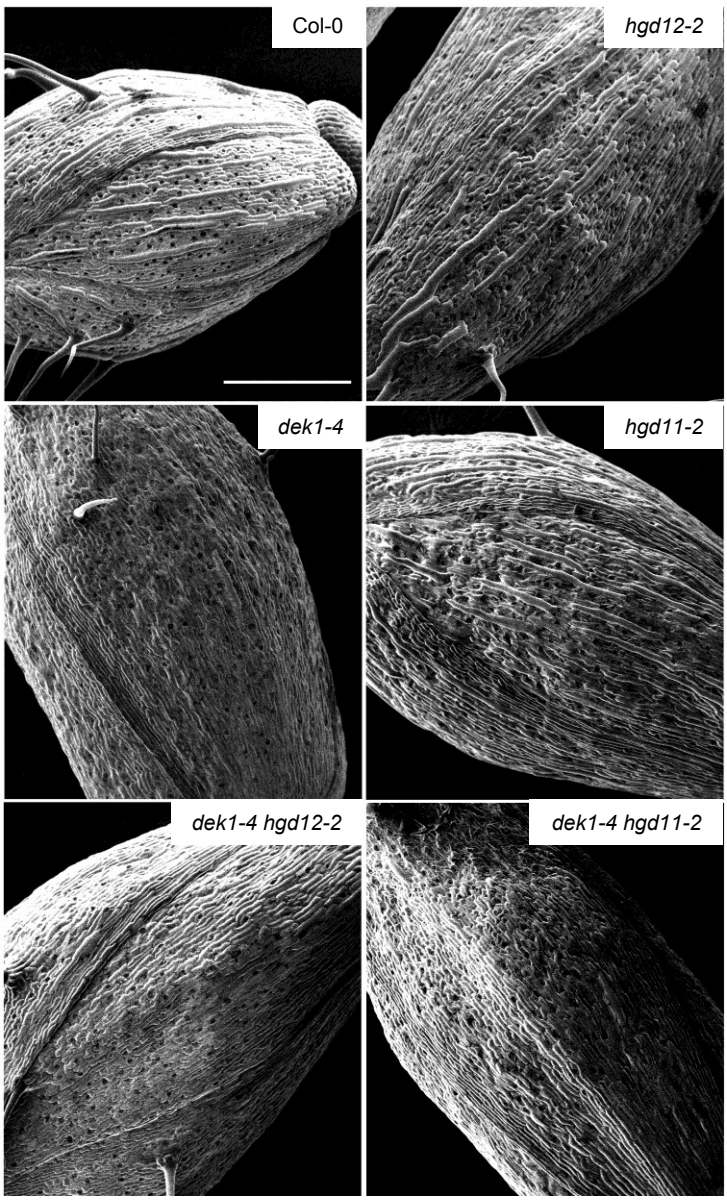

Figure S3 - **Giant cell phenotypes in *hdg11-2, hdg12-2* and double mutants with *dek1-4*.**

Scanning electron microsocopy images of floral buds from double homozygous mutants and parental lines. Bar = 250 µm

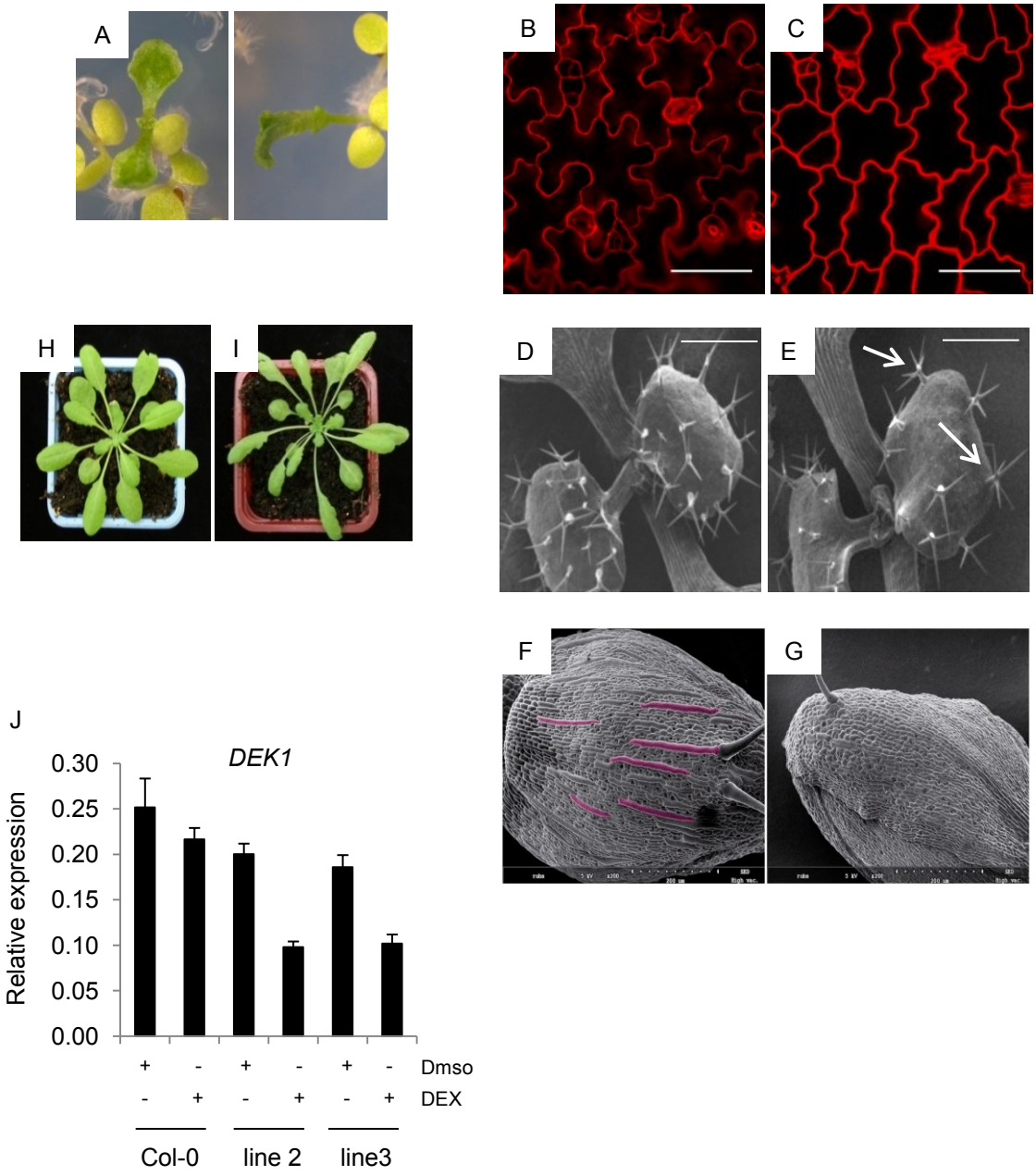

Figure S4 - Phenotypes of *35S:amiRDEK1* plants and *DEK1* expression levels in inducible *amiRDEK1 lines* .

(**A**) Phenotypes of *35S:amiRDEK1* seedlings. (**B** and **C**) representative pictures of the adaxial side of 4-day-old cotyledons. Col-0 (**B**) and *35S:amiRDEK1* (**C**) seedlings were stained with propidium iodide and imaged by confocal microscopy; Bar = 50 µm. Col-0 (**D, F** and **H**) and *35S:amiRDEK1* (**E, G** and **I**) plants. Rosette morphology (**H** and **I**), scanning electron microsocopy images of 10-day-old seedling leaves (**D** and **E**) and floral buds (**F** and **G**). Bar = 500 µm (**D** and **E**) and 200 µm (**F** and **G**). (**J**) *DEK1* mRNA levels in adult leaves were quantified by quantitative RT-PCR and normalized using the expression of the *EIF4A* gene.

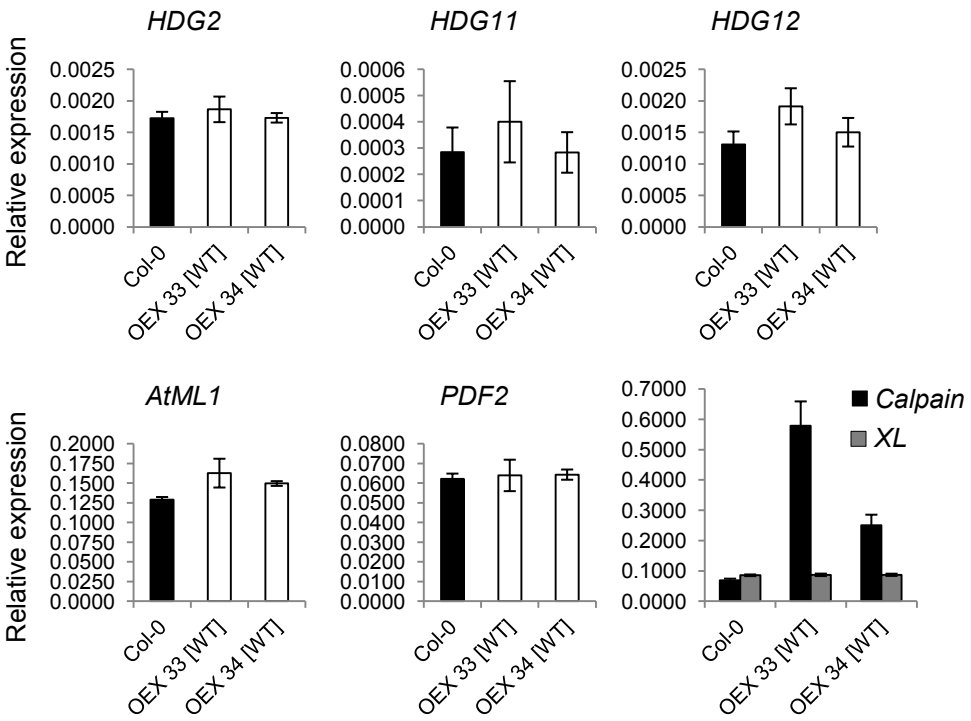

Figure S5 - Over-expression of the *DEK1* Calpain domain does not strongly affect the expression of *HD-ZIP IV*-encoding genes.

Gene expression levels in the aerial parts of 6-day-old Col-0 and two independent Calpain over-expressing lines (*OEX [WT]* line 33 and 34) were quantified by quantitative RT-PCR and normalized using the expression of the *EIF4A* gene. Graph represents the average of three independent biological replicates ± SD. "*XL"* denotes primers detecting transcript from the extracellular loop-encoding region of *DEK1* (endogenous transcripts). "*Calpain"* denotes primers from the Calpain domain of *DEK1* (endogenous + transgenic transcripts).

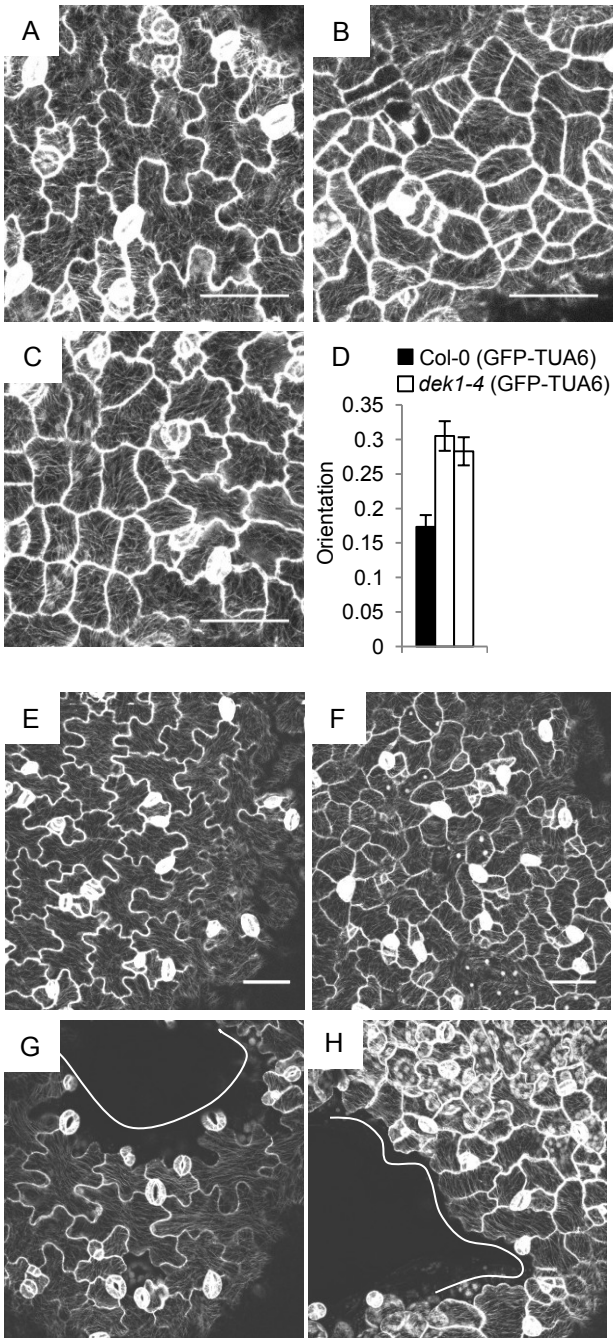

Figure S6 – Cortical microtubule orientation in *dek1-4* epidermal cells.

Z-stacks of confocal images of the adaxial side of seedling cotyledons. Col-0 (**A**, **E**, **G**) and *dek1-4* (**B**, **C**, **F**, **H**) introgressed into a background expressing GFP-TUA6. Bar = 50 µm. (**D**) Quantification of CMT orientation. (**E** and **F**) unwounded cotyledons. (**G** and **H**) cotyledons 6 hours after ablation. White lines demarcate the ablation site.

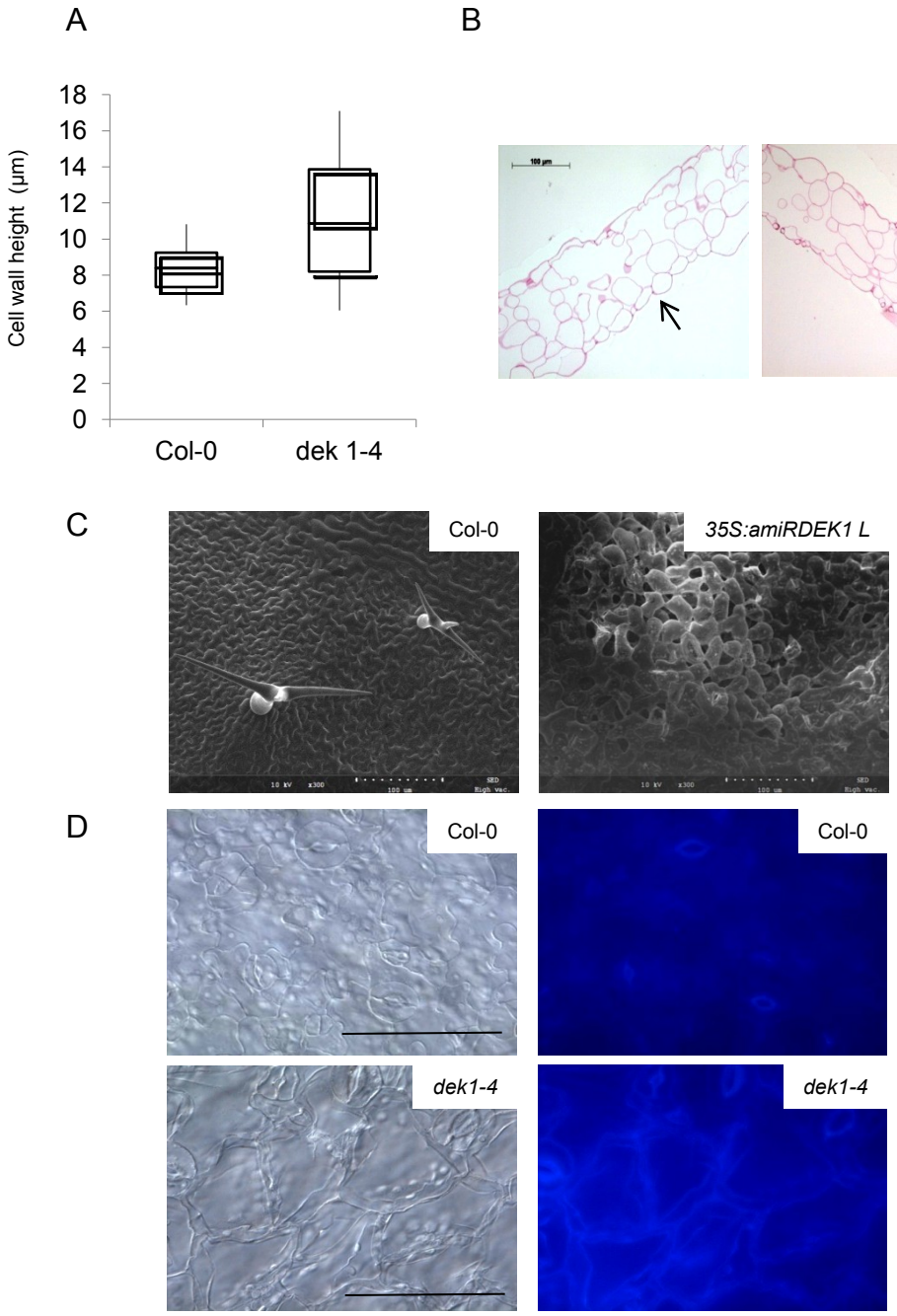

Figure S7 - Analysis of cell-cell junctions in the adaxial epidermis of plants with reduced *DEK1* activity.

For **A** and **B** cotyledons were fixed, sectioned, stained and recorded using a protocol previously described (Xing et al., 2013) and junction lengths (from outer to inner surface of the epidermis) were measured using the straight line function of ImageJ. (**A**) Box plot chart of cell junction height showing median (central bar) and interquartile range (box). *n* = 16 for Col-0 and *n* = 18 for *dek1-4*. (**B**) Representative images. (**C**) Representative SEM pictures of adaxial epidermis of cotyledons from Col-0 and *35S:amiRDEK1 line L* showing cell separation. (**D**) Adaxial epidermis of Col-0 and *dek1-4* 4-day old seedlings stained with aniline blue and imaged either under white light using DIC optics (left) or using a DAPI filter (right). Aniline blue staining was carried out as described in (Galletti et al., 2008). Callose is only present in epidermal cell junctions in *dek1-4*. Bar = 100 µm.

Table S1. Primers

Name	Sequence	AGI code	Description/Purpose
*I miR**DEK1**-s*	GATAACATATTAGGAAAAGCCGGTCTCTCTTTTGTATTCC		Cloning *amiRDEK1*
*II miR**DEK1**-a*	GACCGGCTTTTCCTAATATGTTATCAAAGAGAATCAATGA		Cloning *amiRDEK1*
*III miR**DEK1***s*	GACCAGCTTTTCCTATTATGTTTTCACAGGTCGTGATATG		Cloning *amiRDEK1*
*IV miR**DEK1***a*	GAAAACATAATAGGAAAAGCTGGTCTACATATATATTCCT		Cloning *amiRDEK1*
RG15	CGTCGTGCTGCTTACAACAT	**AT1G55350**	Genotyping *dek1-4* mutation;
DEK1 end Rev	CTACAAAGCTTCAAGAACAA	**AT1G55350**	Genotyping *dek1-4* mutation;
DEK1 Calpain-Fw	AAACAAGAGGGGTTCTTACTTGG	**AT1G55350**	genotyping *dek1-4* mutation*;* qRT-PCR
DEK1 Calpain-Rev	TTCGAATCTGAACAAGTCTGTGC	**AT1G55350**	qRT-PCR
DEK1 XL-Fw	CTTGAGAGAAGGTTTTCGGAG	**AT1G55350**	qRT-PCR
DEK1 XL-Rev	CCTGTTCGAGTTAGATTGTCAG	**AT1G55350**	qRT-PCR
EIF4A FW	TTCGCTCTTCTCTTTGCTCTC	**AT3G13920**	qRT-PCR
EIF4A Rev	GAACTCATCTTGTCCCTCAAGT	**AT3G13920**	qRT-PCR
AtML1-Fw	GGATATACAGGCAGAAGAAAATCGAG	**AT4G21750**	qRT-PCR; used in San-Bento et al., 2013
AtML1-Rev	GATGATACATGATGATGATGGATGC	**AT4G21750**	qRT-PCR; used in San-Bento et al., 2013
PDF2-Fw	CACGAAAATATATTGATCAGTGCCTTG	**AT4G04890**	qRT-PCR; used in San-Bento et al., 2013
PDF2-Rev	CAAACATGTTTGGATGGTACATTGTTA	**AT4G04890**	qRT-PCR; used in San-Bento et al., 2013
HDG2-FW	TCTGGAGAAGTTGGCGTGA	**AT1G05230**	qRT-PCR
HDG2-Rev	AAGCTTATAACCATCCGCTCTG	**AT1G05230**	qRT-PCR
HDG11-FW	TCTCGTGATCTCGGTGGAGT	**AT1G73360**	qRT-PCR
HDG11 -Rev	TCTGAGCAAGTCTCATCATGC	**AT1G73360**	qRT-PCR
HDG12-FW	CCCTTGATCTTGGAGGAGTG	**AT1G17920**	qRT-PCR
HDG12-Rev	CCATTCTGTGAGCAAGTCTCAT	**AT1G17920**	qRT-PCR
SIM-Fw	ACAAGATTCCTCCCACCACA	**AT5G04470**	qRT-PCR
SIM-Rev	GAAGGTGGACGGGGTTTC	**AT5G04470**	qRT-PCR
LGO-Fw	CTCCTCCGCCGAGAAAAC	**AT3G10525**	qRT-PCR
LGO-Rev	ATCATCAGAGCCGCCGTA	**AT3G10525**	qRT-PCR
HBT-Fw	ATGAACCTGGTGCGGAGA	**AT2G20000**	qRT-PCR
HBT-Rev	TTGAGCAGCATTCTTCCTTCT	**AT2G20000**	qRT-PCR
KRP6-Fw	GAAACCGAAACCGAAACCTC	**AT3G19150**	qRT-PCR
KRP6-Rev	CCCTCACTCACTGGACTCGT	**AT3G19150**	qRT-PCR
CYCD3;1-Fw	GCTCACTGGGATTTCCTCAA	**AT4G34160**	qRT-PCR
CYCD3;1-Rev	ACCCGACAAATCTTGAATCG	**AT4G34160**	qRT-PCR
DEL1-Fw	TTGATGACGCTGCAAAATTACT	**AT3G48160**	qRT-PCR
DEL1 Rev	CATAAAGCCGCCTCACTTTAGTT	**AT3G48160**	qRT-PCR
HDG11-LP	GCGTCTTCATCTCGTGATCTC	**AT1G73360**	Genotyping
HDG11-RP	GAAGCAGCAGAACAATTGGAG	**AT1G73360**	Genotyping
HDG12-LP	CTATTCCCCGAGATCTTTTGG	**AT1G17920**	Genotyping
HDG12-RP	TGGCTGAGATGGTAAACTTGG	**AT1G17920**	Genotyping
LBb3.1	ATTTTGCCGATTTCGGAAC		Genotyping